Voltage Dependence of Proton Pumping by Bacteriorhodopsin Is Regulated by the Voltage-Sensitive Ratio of M_1 to M_2

G. Nagel,*# B. Kelety,* B. Möckel,§ G. Büldt,§ and E. Bamberg*#
*Max-Planck-Institut für Biophysik, D-60596 Frankfurt; #Johann Wolfgang Goethe Universität, FB15, Biozentrum, D-60439 Frankfurt; and §IBI-2, Forschungszentrum, D-52425 Jülich, Germany

ABSTRACT The voltage dependence of light-induced proton pumping was studied with bacteriorhodopsin (bR) from *Halobacterium salinarum*, expressed in the plasma membrane of oocytes from *Xenopus laevis* in the range −160 mV to +60 mV at different light intensities. Depending on the applied field, the quenching effect by blue light, which bypasses the normal photo and transport cycle, is drastically increased at inhibiting (negative) potentials, and is diminished at pump current increasing (positive) potentials. At any potential, two processes with different time constants for the M → bR decay of ~5 ms (τ_1) and ~20 ms (τ_2) are obtained. At pump-inhibiting potentials, a third, long-lasting process with $\tau_3 \approx 300$ ms at neutral pH is observed. The fast processes (τ_1, τ_2) can be assigned to the decay of M_2 in the normal pump cycle, i.e., to the reprotonation of the Schiff base via the cytoplasmic side, whereas τ_3 is due to the decay of M_1 without net pumping, i.e., the reprotonation of the Schiff base via the extracellular side. The results are supported by determination of photocurrents induced by bR on planar lipid films. The pH dependence of the slow decay of M_1 is fully in agreement with the interpretation that the reprotonation of the Schiff base occurs from the extracellular side. The results give strong evidence that an externally applied electrical field changes the ratio of the M_1 and the M_2 intermediate. As a consequence, the transport cycle branches into a nontransporting cycle at negative potentials. This interpretation explains the current-voltage behavior of bR on a new basis, but agrees with the isomerisation, switch, transfer model for vectorial transport.

INTRODUCTION

Proton pumping by the light-driven pump bacteriorhodopsin from *Halobacterium salinarum* creates an electrochemical potential of up to −280 mV inside the cell (Michel and Oesterhelt, 1976). The electrochemical potential is used for ATP synthesis and is coupled to other secondary active transporters in the plasma membrane. Detailed information about the structure and function of bR has been obtained in the past by a variety of biochemical and biophysical methods. A substantial help to understanding the pumping mechanism was the determination of the three-dimensional structure (Henderson et al., 1990; Grigorieff et al., 1996). bR consists of seven α-helices (A, B, C, D, E, F, G) forming a transmembrane channel-like structure. The channel consists of the helices B, D, F and G and is divided into a cytoplasmic (CP)- and an extracellular (EC)-oriented half-channel by the chromophore retinal, which is bound via the Schiff base to lysine 216 in helix G.

Light-driven proton translocation is closely connected to the photocycle of bR. After excitation, retinal isomerizes from all-*trans* to 13-*cis* and forms, via the J, K, and L intermediates, the blueshifted M product. During the formation of M_{cis} (the subscript describes the configuration of the retinal), the proton is released from the Schiff base via Asp^{85} to the extracellular side, and the pK of the Schiff base is shifted from an original pK of >13 to pK < 4.0 (Druckmann et al., 1982; Sheves et al., 1986). Still in M_{cis}, the pK shifts again to pK > 10, and the proton is taken up via Asp^{96} from the intracellular side. This process of changing accessibility of the Schiff base for protons from EC to CP can be called a molecular switch (Mathies et al., 1991; Oesterhelt et al., 1992; Haupts et al., 1997; Lanyi, 1995; Lanyi and Váró, 1995), whereby M_{cis} is subdivided into M_1 (with proton accessibility to EC) and M_2 (with proton accessibility to CP). The underlying molecular events for the switch are either conformational changes in the protein and/or changes on the retinal configuration (Schulten and Tavan, 1978). Spectroscopic and structural analysis of the kinetics of the photocycle gave evidence for the existence of the two M states, where the M_1 to M_2 transition is the irreversible step in the transport cycle (Korenstein et al., 1978; Váró and Lanyi, 1991a,b; Koch et al., 1991; Sass et al., 1997).

Recent studies on the vectorial transport of Asp^{85} bR mutants, the light-driven chloride pump halorhodopsin, and sensory rhodopsin I resulted in a general model for the description of the different observed transport modes of the retinal-binding proteins (Oesterhelt et al., 1992; Bamberg et al., 1993; Tittor et al., 1994; Haupts et al., 1997). For wild-type bR, the M_1-to-M_2 transition represents the molecular switch that is the key step in vectorial transport.

Important aspects of this process, the regulation of the pump by an external field and the underlying molecular events, are not understood, although many efforts have been made with time-resolved spectroscopy or electrical studies to solve these problems. All of these studies, including the spectroscopic work, were carried out under short-circuit conditions at zero or undefined membrane potentials, or on

Received for publication 10 July 1997 and in final form 15 October 1997.
Address reprint requests to Dr. Ernst Bamberg, Max Planck Institute of Biophysics, Kennedyallee 70, D-60596 Frankfurt am Main, Germany. Tel.: 49-69-6303-300/301; Fax: 49-69-6303-305; E-mail: bamberg@biophys.mpg.de.

0006-3495/98/01/403/10 $2.00

systems with unsatisfactory orientation of bR in the respective membrane system.

An influence of preillumination of bR in whole cells or proteoliposomes on the M decay was reported (Quintanilha, 1980; Dubrovskii et al., 1983), showing that the light-induced potential retards the M decay up to a factor of 10. The results are summarized in a paper by Westerhoff and Danczházy (1984), where a reprotonation of the Schiff base is assumed to occur from the outside, representing the slow M decay, or the N $\rightarrow$ M back-reaction in the photocycle. This could be suggested by the result that the M decay appears to be biexponential, where the amplitudes of the different processes change with the applied electrical field (Groma et al., 1984).

Electrical studies were performed on dried purple membrane samples (Váró and Keszthelyi, 1983; Lukashev et al., 1980), on bR proteoliposomes, on bR adsorbed to millipore filters (Hellingwerf et al., 1978), and on bR incorporated into planar lipid membranes (Bamberg et al., 1980; Braun et al., 1988). In all of these studies, an electrical potential directed against the proton pumping diminished the pump current. The photoelectrical studies could be performed only under unsatisfactory experimental conditions, because no appropriate system was available to study the transport properties of the pump under well-defined voltage-clamp conditions.

Recently we succeeded in expressing bR in the plasma membrane of oocytes from *Xenopus laevis*, which allows the investigation of light-induced pump currents under voltage-clamp conditions (Nagel et al., 1995). Here we show that the voltage dependence of the pump current can be explained by the potential dependence of the ratio between M_1 and M_2, demonstrating the significance of the two M states for the vectoriality of the proton pumping process. The conclusions drawn from these experiments are supported by complementary results obtained on planar lipid membranes.

MATERIALS AND METHODS

Enzymes and reagents

Restriction enzymes were obtained from New England Biolabs. Calf intestine phosphatase and T4 DNA ligase were obtained from Boehringer Mannheim. Fragments used for ligation were separated on agarose gels and purified by use of the QIAEX kit from QIAGEN (Hilden). The T7-Cap scribe kit was obtained from Boehringer Mannheim. Salts were p.a. grade and were obtained from Merck (Darmstadt). EGTA, HEPES, 3-(*N*-morpholino)propanesulfonic acid, and retinal were from Sigma. The UV light-insensitive protonophore 1799 (2,6-dihydroxy-1,1,1,7,7,7-hexafluoro-2,6 bis(trifluoromethyl)heptane-4-one) was obtained from Dr. P. Heytler (Du Pont Nemours).

Preparation of plasmid DNA and cRNA synthesis

Plasmid pGEMHE, a derivative of pGEM3z (Promega, Madison, WI), was used for in vitro generation of cRNA transcripts. Plasmid pGEMHE contains the 3′ and 5′ untranslated regions of the β-globin gene from *Xenopus*. A promoter-free bop gene, encoding bacterioopsin (including its signal sequence), was isolated from pBSbop by cleavage with *Bam*Hl and *Hin*dIII and ligated into pGEMHE, behind the T7 RNA-polymerase promoter. *Escherichia coli* was transformed by the RbCl method. Plasmids from *E. coli* were isolated by the method of Birnboim and Doly (1979). *Nhe*I-linearized plasmid DNA was used for the in vitro generation of cRNA with the T7-cap scribe kit.

Oocyte microinjection and incubation

Oocytes were prepared as described elsewhere (Grygorzcyk et al., 1989), in short: 50 nl cRNA (100 to 400 ng/μl) was injected per oocyte. Expression seemed to saturate above 10 ng. The oocytes were incubated for 3–5 days at 18°C with 1 μM retinal in the medium to reconstitute the bR from bacterioopsin. After ~4 days at 18°C, the level of expression became constant and the measured pump currents did not show any further increase. A previous estimation showed that ~100 molecules μm^{-2} appear in the plasma membrane (Nagel et al., 1995).

Voltage-clamp experiments

To determine the light-induced pump currents, a two-electrode voltage clamp amplifier (Turbo TEC-05; npi, Germany) was used. Voltage pulses between −160 mV to +60 mV were applied. The sign of the applied potential is assigned according to the usual convention, i.e., with reference to the bath electrode (e.g., −100 mV holding potential means that the inside of the bath is 100 mV more negative). All current recordings were filtered at 350 Hz and are presented with the usual convention, i.e., outward electrical current is positive (upward).

The oocyte was illuminated with a 75-W high-pressure xenon arc lamp (Osram XBO 75) and filtered through an IR-filter and a short-wavelength cutoff filter (GG495 = "green"), or a continuous He-Ne laser (633 nm = "red") and a continous He-Cd laser (442 nm = "blue") were used. To activate the pump, the light was focused on the oocyte for a short time (200–600 ms). The maximum light intensity was 2 W/cm^2 for the xenon lamp, 3 W/cm^2 for the "red" laser, and 1 W/cm^2 for the "blue" laser. Red light instead of the usual green light was applied when two lasers were required to focus the light on the same spot on the oocyte to study the effects of blue light. Previously we determined an action spectrum for bR in oocytes (Nagel et al., 1995), showing ~50% efficiency at 633 nm compared to the maximum at ~570 nm. Therefore, the maximum light intensity used (of the "red" laser) was relatively high.

To minimize the offset current due to the variety of channels and transporters in the oocyte membrane, the bath solution contained 90 mM NaCl, 20 mM TEA-Cl, 5 mM $BaCl_2$, 0,5 mM $CdCl_2$, 10 mM MOPS (pH 7.6). The pipette filling solution was 3 M CsCl, 0.6 M TEA-Cl, or 3 M KCl.

Control voltage-clamp experiments

As a control, cRNA-injected oocytes were also incubated without retinal showing 10% (at maximum) of the pump currents, indicating the reconstitution of bacterioopsin with endogenous retinal. The incubation with retinal did not change the effects of light on uninjected oocytes.

Because the oocytes are pigmented, control experiments have also been carried out with uninjected or water-injected oocytes to detect possible light-induced heat effects on the membrane conductance. Indeed, depending on the applied potential, a small photoeffect could be observed in oocytes not injected with cRNA. Red and blue light cause a small but distinct light-induced effect on uninjected oocytes. The effect is less than 2% of the observed pump current at zero potential and, contrary to the bR signal, the direction of this light artifact shows the direction of the applied electrical field (data not shown). Therefore, this small light artifact was normally neglected, but, as its contribution increases at extreme negative voltages and with illumination by two cw lasers, it had to be taken into account for the data evaluation in Fig. 3 *b*.

Planar lipid bilayer experiments

Optically black lipid membranes with an area of $\sim 10^{-2}$ cm^2 were formed in a Teflon cell filled with a specified electrolyte solution (1.5 ml in each compartment). The membrane-forming solution contained 1.5% (w/v) diphytanoyl lecithin (Avanti Biochemicals, Birmingham, AL) and 0.025% (w/v) octadecylamine (Riedel-de-Haen, Hannover, Germany) in *n*-decane to obtain a positively charged surface (Dancsházy and Karvaly, 1976). Purple membrane suspensions ($OD_{568} = 10$) were sonicated for 1 min in a sonication bath, and aliquots of 20 μl were added, with stirring, to the rear compartment. Photosensitivity of the compound membrane developed in time and reached the maximum value after ~40 min. The membrane was illuminated with a 100-W mercury lamp (Osram HBO 100) and filtered through specified filters, or by light from a dye laser (Lambda Physics; 10-ns pulse length tuned to the specified wavelengths: 580 nm when the dye rhodamine 6G was used (LC5900 from Lambda Physics, peak at 581 nm) or 400 nm when the dye PBBO was used (LC4000 from Lambda Physics, peak at 396 nm)). The irradiance of the continuous light source was up to 2 W/cm^2 when filtered through heat-protecting glass and a 495-nm cutoff glass filter. The laser light pulse energy was varied between 0 and 500 μJ. To avoid photo-artifacts, the membrane cell was connected to an external measuring circuit via Ag/AgCl electrodes, which were separated from the Teflon cell by salt bridges. The stationary current was measured with a current amplifier (Keithley; model 427), whereas for the kinetic measurements a custom-made current-voltage converter was used. The time resolution in the kinetic experiments was ~5 μs. The purple membrane and the planar film are capacitively coupled, so that the capacitive current can be described as

$$I(t) = I_0 \cdot \exp\left(-\frac{t}{\tau}\right) \qquad I_0 = I_{P0} \cdot \frac{C_M}{C_M + C_P} \qquad \tau = \frac{C_M + C_P}{G_M + G_P}$$

where I_0 is the initial current at time 0, I_{P0} is the pump current in the stationary state at zero potential, and τ is the system time constant of the compound membrane system. A scheme of the experimental situation (which also explains C_M, C_P, G_M, and G_P) is given in Fig. 1.

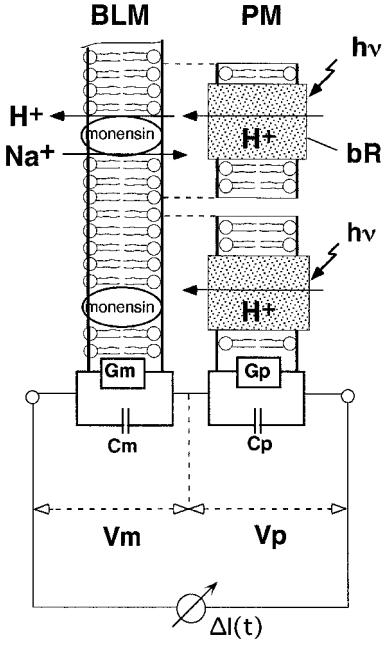

FIGURE 1 Schematic representation of the compound membrane (purple membrane, black lipid membrane), G_m and G_P represent the conductance of the BLM and the purple membrane, respectively. C_m and C_P represent the corresponding capacitances.

The system time constant τ_o of the compound membrane was determined to be 0.9 s. A single 570-nm flash of 10-ns duration was applied, so that a single turnover of bacteriorhodopsin was measured, followed by the discharging of the membrane capacitors. This means that within a time window determined by the resolution of the measuring amplifier (~5 μs) and the discharging time of the capacitors, the charge movement of bacteriorhodopsin can be determined. The observed currents always have the same direction, showing that the protons are pumped in the direction of the protein-free side, in agreement with our earlier observation that the purple membrane binds preferentially with its extracellular side to the black lipid membrane (e.g., Bamberg et al., 1979; Fahr et al., 1981; Tittor et al., 1994).

RESULTS

Oocyte experiments

Previously we have shown that in the voltage range −165 mV to +60 mV, the light-induced pump current is always outwardly directed (Nagel et al., 1995). This indicated a perfect orientation of the bR molecules in the plasma membrane, leading to outwardly directed net proton transport.

Fig. 2 demonstrates the voltage dependence of stationary pump currents at different light intensities. Between −160 mV and +60 mV, the amplitude of the current varies by more than a factor of 4 at high light intensity (~2 W/cm^2). At low light intensity (~0.02 W/cm^2), the current becomes voltage independent at more positive potentials, i.e., the absorption of photons becomes rate limiting. Linearly extrapolating these data in the negative voltage range would lead to a completely inhibited pump current at a potential of ~−250 mV.

The current-voltage behavior raises the question: What is the reason for the reduction or increase of the pump current by the voltage? Which step in the photocycle is mainly affected? The analysis of photocurrent kinetics has demonstrated that the main charge movement occurs during the M → bR decay (Drachev et al., 1981; Keszthelyi and Ormos, 1980; Fahr et al., 1981). Therefore, it is plausible to assume that this step is the crucial process that is regulated by the externally applied electric field.

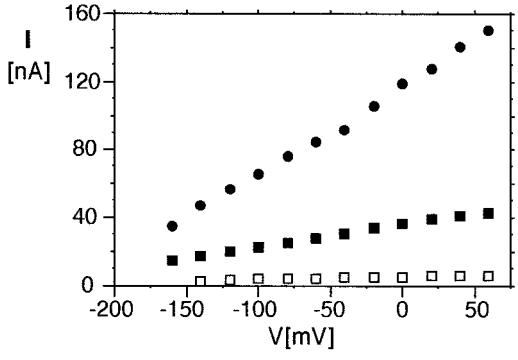

FIGURE 2 Current-voltage behavior of bR expressed in oocytes at different light intensities. Light source: XBO 75 with heat filter and GG495 cutoff filter (495 nm < λ < 740 nm), 200-ms flashes. ●, 2.0 W/cm^2; ■, 0.2 W/cm^2; □, 0.02 W/cm^2

Fig. 3 *a* shows pump currents at different applied potentials under red light and red and blue light conditions. The baseline is dependent on the applied potential, indicating conductance changes of the oocyte membrane. Nevertheless, the light response can be detected with high accuracy and reproducibility on the same cell. The off response (in Fig. 4 *a*) of the red light-induced pump current shows two relaxation times of ~5 ms and ~20 ms, virtually independent of the applied voltage. Only the amplitude of the fast process vanishes at pump current-inhibiting potentials. This implies that the time course of the M decay is virtually unaffected by the electric field. A similar effect for the amplitude of the M state was found by time-resolved spectroscopy by Groma et al. (1984).

Fig. 3 *a* also shows the effect of additional blue light illumination on the red light-induced pump current, demonstrating the well-known quenching effect of blue light. The underlying molecular mechanism is the photoisomerization of 13-*cis* retinal to the all-*trans* form in the M state, which is followed by the reprotonation of the Schiff base from the extracellular side. Spectroscopically, this effect was observed first by Oesterhelt and Hess (1973), whereas the inhibition of the proton transport by blue light was demonstrated originally by Ormos et al. (1978). Thus the blue light effect is a measure of the concentration of the M intermediate, because the photocycle is short-circuited after absorption of an additional blue photon in the M state. Therefore, the voltage dependence of the quenching effect on the photocurrent caused by additional blue light was studied.

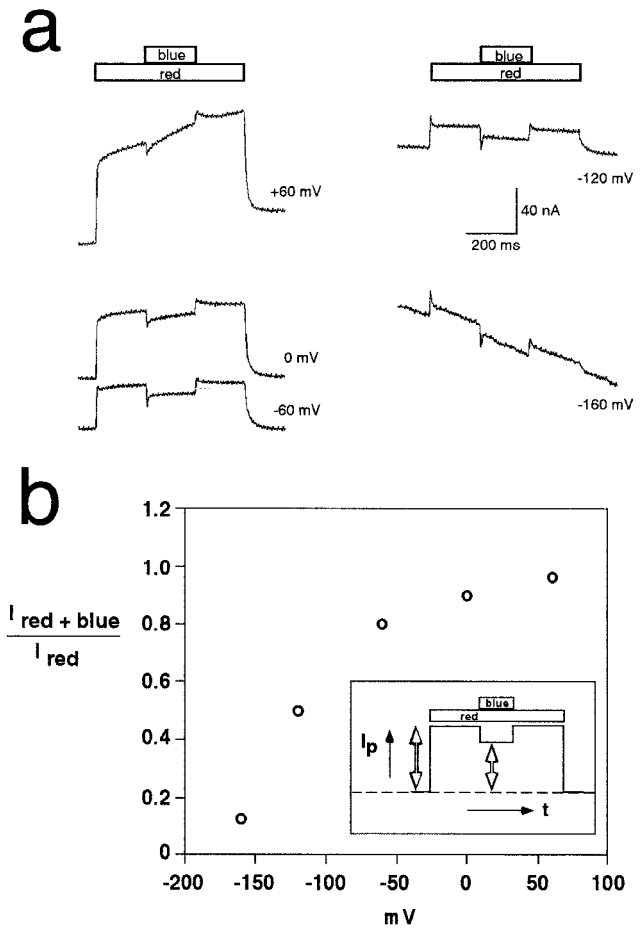

FIGURE 3 (*a*) Blue light-induced quenching of the pump current depending on the applied potential. Red, illumination with He-Ne laser (633 nm, 3 W/cm^2); blue, illumination with He-Cd laser (442 nm, 1 W/cm^2). (*b*) Evaluation of the voltage-dependent blue light effect. The inset shows a schematic of the evaluation procedure.

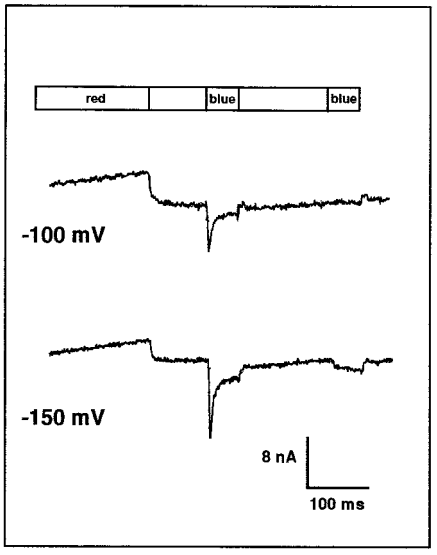

FIGURE 4 Traces from double-flash experiments at two different holding potentials, showing the increased lifetime of M. Red light intensity, 3 W/cm^2; blue light intensity, 1 W/cm^2. At different time intervals Δt, the amount of M was measured by the blue light-induced transient current caused by the reprotonation of the Schiff base from the extracellular side. The second blue light flash was given for control and the response is time independent, showing the light-induced conductance change, as discussed in Materials and Methods.

As can be seen, the quenching effect increases drastically when the applied electrical field is changed from positive to negative potentials. At −160 mV, the stationary current is almost completely quenched by blue light, but no inverted pump current can be observed. However, the larger the applied negative potential, the larger the transient current, which indeed is of opposite direction. This phenomenon of the transient currents in both directions will be discussed below. Fig. 3 *b* represents the evaluation of the quenching effect, where the white (red + blue) light-induced pump current divided by the red light-induced current is plotted against the applied potential. The quenching effect disappears toward positive potentials, whereas at large hyperpolarizing potentials the white light-induced current is only a small fraction of the red light-induced one. The *I*/*V* relation, therefore, is obviously dependent on the wavelength of the activating light.

Because the blue light-induced quenching of the pump current depends strongly on the externally applied electrical field, we investigated the M decay in the following way. As blue light induces a *cis-trans* isomerization of the retinal in the M state, followed by the reprotonation of the Schiff base

from the extracellular side, a transient current directed against the normally outwardly flowing proton pump is obtained. Therefore, the amplitude of the blue light-induced current reflects the amount of M. In a series of double-flash photoelectrical experiments, the amount of M was measured by a pulse of blue light after the red light was switched off at different time intervals. A surprising result was obtained.

Fig. 4 shows such an experiment at −100 mV and −150 mV, respectively. As can be seen directly, the M state seems to be arrested by the applied potential, because 100 ms after switching off the red light, a blue light-induced transient current can still be observed. The stationary component in the figure is the artifact discussed in Materials and Methods and is subtracted, when present, from the bR-induced signal. The transient current reflects the reprotonation of the Schiff base from the extracellular side. The higher the applied electrical field against the direction of the pump, the larger the blue light-induced amplitude of this current. Fig. 5, *a* and *b*, represents the amplitude of the blue light-induced current at three different voltages, depending on the time interval Δt. As can be seen from Fig. 5 *b*, where the three curves from Fig. 5 *a* are normalized, the time course is independent of the applied voltage. A third increased M decay time of ~300 ms is observed in addition to the usual ~5 and ~20 ms. This means that the M state, probably M_1, is arrested by the electrical field. This long lifetime of M explains the reduction of the pump current by the negative potential, whereas the increase in the current at positive potentials is due to the reduced population of the M_1 state demonstrated by the reduction of the quenching effect. At zero or low voltages, where the pump cycle is ≤20 ms, no such effect could be detected within the time resolution for the double-flash experiments (25 ms). Oocytes not injected with RNA and incubated with retinal showed no or negligible blue light-induced currents, which, if present, however, are not time or voltage dependent and are not induced by the red light preillumination.

The results suggest that the applied electric field induces a different pathway for the reprotonation of M via the extracellular half-channel (EC). If hyperpolarizing potentials acted on the $M_2 \rightarrow BR$ reactions (the main electrogenic events in the transport cycle; Drachev et al., 1981; Keszthelyi and Ormos, 1980; Fahr et al., 1981), one would find a continuously slowing down of the M decay with increasing negative potentials. This was not found. Both processes, the fast components (the decay of M_2 with ~5 and ~20 ms) and the slow process (presumably the decay of M_1), change only in amplitude but not the time course by variation of the externally applied electric potential.

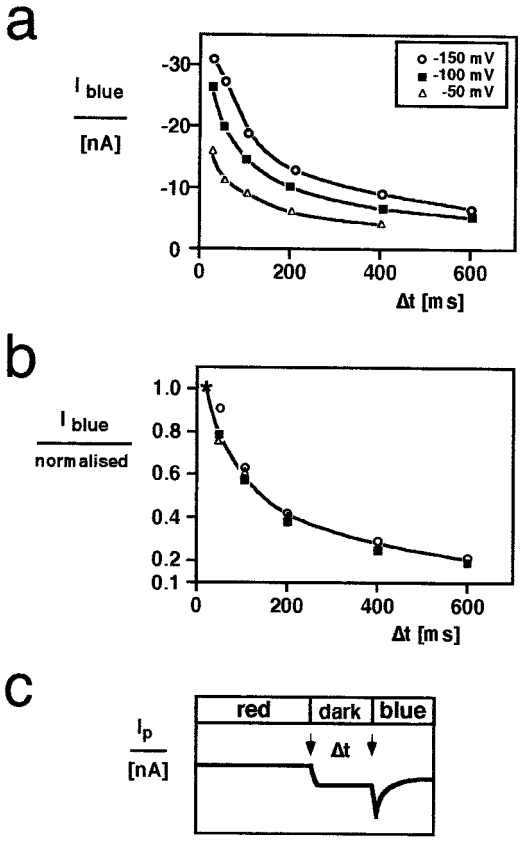

FIGURE 5 Evaluation of the M decay at three different potentials. (*a*) Amplitudes of blue light-induced transient inward currents at different delay times Δt. (*b*) Normalized M-decay as demonstrated in *a*. (*c*) The scheme shows the evaluation procedure.

Black lipid membrane experiments

As shown above, the slow M decay only becomes relevant at negative potentials. To understand the slow kinetics of the thermal decay of the M intermediate, one would suggest that the reprotonation of the Schiff base occurs from the extracellular side. This is realistic because at neutral pH and the low pK of the Schiff base in the M_1 state, which is presumably arrested by the negative potential, the reprotonation is slow because of low proton concentration. Therefore, the lifetime of M_1 should strongly depend on the pH.

With the oocyte system it is difficult to measure pH dependencies, because only the external pH can be controlled, so that a pH gradient will be imposed that might change during the experiment. Therefore, we used the black lipid membrane technique to study the pH effect. Here the pH can be changed symmetrically on both sides of the purple membrane.

When purple membranes are adsorbed in an oriented manner to planar lipid membranes, light-induced transient currents are observed via the capacitive coupling between the purple membrane and the planar lipid membrane. These currents create a potential V_P across the purple membrane and a potential V_M across the covered planar lipid bilayer, because of the charging of the corresponding capacitances of the purple membrane and the planar lipid bilayer, respectively (C_P, C_M). Under short-circuit conditions, V_p equals $-V_M$. Under stationary illumination, the potential V_p produced by the pump current is built up with the characteristic RC time of the compound membrane, corresponding to the

decay time of the capacitive current. After the light is turned off, V_p vanishes with the system time constant τ_0 (see Materials and Methods). The system time constant τ_o of the compound membrane was determined to be 0.9 s. The experimental situation is shown schematically in Fig. 1. Details are given in Bamberg et al. (1979).

To avoid a possible pH gradient effect on bR by the accumulation of protons in the interstitial space between the purple membrane and the underlying lipid membrane, the electroneutrally Na^+/H^+ exchanging ionophore monensin was applied, so that an acidification within the sandwich-like membrane system can be excluded.

As mentioned above, the potential does not remain constant after the light is switched off. However, a qualitative result on the pH dependence of the thermal decay of M_1 can be obtained, as long as this reaction does not exceed the intrinsic membrane time constant of 0.9 s. This is justified, because in the oocyte experiment only the amplitude of the M_1 decay is voltage dependent; its time constant is not.

Fig. 6 shows the disappearance of the bR_{568} state and the appearance of the M state. Both the bR_{568} state and the M state were probed by laser pulse-induced photocurrents before, during, and after a green background light flash with a duration of 250 ms. Trace a shows the transient photocurrent induced by the green background light pulse. Trace b shows the disappearance of the 580-nm laser light-induced current when probed during the 250-ms time interval. After the background light was turned off, the photocurrent recovered with kinetics of several 100 ms. Concomitant with the decrease in the photocurrent under green light, an oppositely directed current induced by blue laser pulses (400 nm) can be observed (trace c). After the background light is turned off, these currents disappear with kinetics similar to those of the recovery of the 580-nm laser-induced currents. As can be seen in Fig. 6, trace b, the 580-nm laser-induced currents do not recover completely. Further evaluation shows a second time constant for the complete recovery of ~16 s. The reason for this is unclear, because the kinetics of the M decay probed by blue light-induced currents are not affected (trace c). A tentative interpretation is that the potential produced by the pumping process generates a repulsive effect between purple membrane and planar lipid bilayer, yielding a looser tight capacitive coupling. When the light is turned off, however, the very slow kinetics might be due to the readsorption of purple membranes to the lipid bilayer. Experiments in the presence of protonophores, where the potential is abolished, support this interpretation, because under such conditions no relaxation in this time domain was observed.

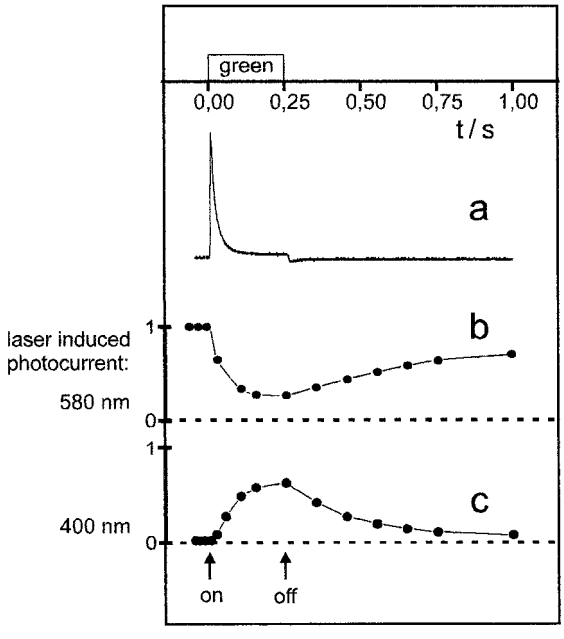

FIGURE 6 Disappearance of the bR_{568} state and concomitant appearance of the M state, probed by a 580-nm and a 400-nm laser pulse, respectively. The membrane area was illuminated with a 0.25-s flash, GG 495 cutoff filter. Green light intensity, 0.1 W/cm^2; electrolyte, 100 mM NaCl, 10 mM Tris-HEPES, pH 7.2. The upper trace shows the illumination by the mercury lamp. (*a*) Green light-induced capacitive photocurrent. (*b*) The 580-nm laser-induced current. (*c*) The 400-nm laser-induced photocurrents. The amplitudes of the laser pulse-induced currents are normalized to 1. The bandwidth of the amplifier was limited to 10 kHz, so that the fast photocurrent response due to the isomerization process of the chromophore was not observed.

Fig. 7 shows an experiment on the lipid bilayer for the determination of the slow M decay. The double-flash protocol is similar to that on the oocytes. First the compound membrane is charged by a green light pulse (5 s). After the light is switched off, a 400-nm, 10-ns laser pulse is applied at different time intervals Δt for the detection of M. Again, as shown for the oocytes, blue light induces an oppositely directed transient current. The amplitude of the current disappears with a characteristic time constant of 140 ms at pH 6 (Fig. 7 *a*). As can be seen in the same figure at pH 8, the time constant increases to 715 ms, showing at least qualitatively that upon lowering of the H^+ concentration, the reprotonation of the Schiff base is slowed down, as expected for a reprotonation from the extracellular side. After addition of the electrogenic protonophore 1799, the blue light-induced currents disappear after the green light is turned off. The uncoupler abolishes V_m and V_p, so that no voltage-induced accumulation of M_1 can be observed.

To confirm that the thermal reprotonation of the Schiff base occurs via the extracellular side, we used mutant D85E, where in the extracellular channel Asp^{85} is exchanged by a glutamate. It has been shown that Asp^{85} is the acceptor for the proton from the Schiff base and therefore is important for the H^+ pumping process (Butt et al., 1989; Gerwert et al., 1990). In mutant D85E the pK of the glutamate carboxylic group is increased, which should increase the buffer capacity in EC (Richter et al., 1996a,b), so that a weaker pH dependence for the M_1 decay is expected. As can be seen from Fig. 7 *b*, the M_1 decay is unaffected by a pH change from 6 to 8 in mutant D85E. The experiment strongly supports the interpretation in the previous sections that the Schiff base is reprotonated via the EC channel and

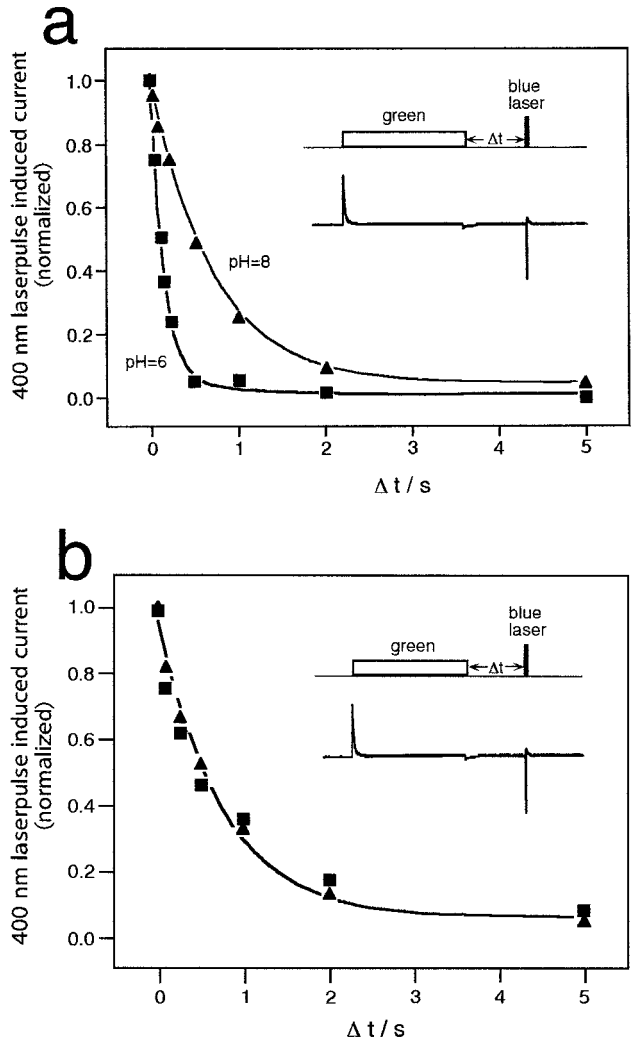

FIGURE 7 M decay in WT bR and the mutant D85E. (*a*) The 400-nm laser pulse-induced response in WT bR at pH 6 (■) and pH 8 (▲) (10 ns, 5 mJ). Green light intensity, 0.1 W/cm^2; electrolyte, 100 mM NaCl, 10 mM Tris-HEPES. The inset shows the double-flash experiment with the transient photocurrents. (*b*) Experiment similar to that shown in *a*, but instead of WT bR, the mutant D85E was used.

that Asp^{85} also plays a central role in the reprotonation of the Schiff base at negative potentials.

DISCUSSION

We have described experiments with bacteriorhodopsin, heterologously expressed in oocytes of *Xenopus laevis*, and complementary experiments with purple membrane sheets adsorbed to a bilayer membrane. Although the bR-oocyte system is new (Nagel et al., 1995) and no photocycle measurements are available for this system, we are quite confident about the relevance of the obtained data for bR in its natural membrane for the following reasons:

1. The data from the oocyte system were confirmed by BLM experiments with adsorbed purple membrane sheets, a well-established technique for functional measurements on bR (Bamberg et al., 1979).

2. Bacteriorhodopsin, heterologously expressed in the fission yeast *S. pombe*, showed absorption and electrical characteristics very similar to those of bR from purple membrane sheets (Hildebrandt et al., 1993).

3. The potential where light-induced proton pumping should cease in oocytes (~ -250 mV, as obtained from extrapolation of the *I*/*V* in Fig. 2) is in good agreement with measurements of bR-generated electrochemical potentials, generated in a more native environment (Michel and Oesterhelt, 1976).

The experiments described in the previous section demonstrate that the two M intermediates play the key role in the voltage dependence in the transport cycle of bR. At hyperpolarizing potentials, an increase in the M_1 concentration was found concomitantly with an additional slow process for the M_1 decay. However, the different time constants for the M-decay seem to be voltage insensitive; only their relative amplitudes vary with voltage. This is surprising, because it has been shown that 80% of the total transported charge is translocated during the M decay (Keszthelyi and Ormos, 1980; Butt et al., 1989; Drachev et al., 1981). However, our results are in agreement with experiments on the determination of the M decay by Groma et al. (1984). The M-decay in cell envelope vesicles is governed by two processes in the millisecond range, where the voltage only influences the relative amplitudes. As discussed by these authors, a second parallel pathway for the M decay appears to be possible. The potential-dependent kinetics are also interpreted as a reprotonation of M via the extracellular side under the effect of hyperpolarizing potentials (Westerhoff and Dancsházy, 1984).

Recently Haupts et al. (1997) presented the so-called IST model (isomerisation, switch, transfer) to explain all known transport modes of the bacterial retinal proteins bR, HR, and SR1. Here the described voltage dependence of bR represents an important test for this model.

The model was developed on the basis of several photoelectrical experiments on planar lipid membranes, where the vectoriality of the proton transport by BL mutants can be reversed, depending on the light conditions (Bamberg et al., 1993; Tittor et al., 1994; Haupts et al., 1996). For wild-type bR, the following scheme was obtained:

$$BR_{trans} \xrightarrow{H^+ \text{ to EC}} M_{1cis} \xleftrightarrow{\text{switch}} M_{2cis} \xrightarrow{H^+ \text{ from CP}} BR_{trans}$$

$$pK_{SB} < 5 \quad pK_{SB} \geq 13$$

The scheme (Oesterhelt et al., 1992; Haupts et al., 1997) contains three elements: the isomerization of the chromophore, the switch, and the transfer of the proton. The switch describes the change in accessibility of protons to the Schiff base. A detailed description of the model is given by Haupts et al. (1997). For WT-bR, the light-induced isomerization is followed by the proton release from the Schiff

base to the extracellular side (EC), forming the M_1 intermediate (with a pK $<$ 5) of the Schiff base. The switch changes the accessibility of the Schiff base to the cytoplasmic side, concomitant with an increase in the pK to a value greater than 13. In the next step, the proton is taken up via CP to the Schiff base under the formation of the intermediate N. N decays under reisomerization via the O intermediate to the ground state.

According to the IST model, the voltage dependence of proton pumping in bR can be explained as follows. The switch that regulates the distribution between M_1 and M_2 is voltage dependent. This is responsible for the voltage dependence of the proton transport. The Schiff base in M_1 is accessible to EC for protons, and its pK is lowered to values smaller than 4, which yields the deprotonation of the Schiff base and the release of the proton to the extracellular side. If, however, the applied electrical field increases the concentration of M_1, the probability of reprotonating the Schiff base from EC is also increased. M_1 still partially undergoes the transition to M_2, which decays via N and O to the ground state, completing the photocycle by the reprotonation via CP. The reprotonation of the Schiff base in M_1, however, is slow because of the low pK of the Schiff base and the low proton concentration at neutral pH. Because of the low proton concentration, the reprotonation step is rate-limited by diffusion and, therefore, becomes voltage independent. One can predict that with increasing concentration of protons, the rate of the reprotonation in M_1 should be increased. Under voltage clamp conditions on the oocytes, such an experiment can only be performed by creating an additional pH gradient, because only the external side is accessible for pH variation. The results on the black lipid membranes show, qualitatively, the correct pH dependence of the slow decay. For wild-type bR, the M decay is accelerated from $\tau = 740$ ms to 140 ms upon lowering of the pH from 8 to 6. The expected factor of 10 per pH unit was not found. This might be due to the residual buffering capacity of Asp^{85} in the EC channel. The result obtained with mutant D85E in the bilayer membrane experiment supports this interpretation. Between pH 6 and 8, indeed no change in the M_1 decay could be observed. The increased pK of glutamic acid as shown recently by Richter et al. (1996a,b) yields a higher buffer capacity.

The results with mutant D85E show unambiguous evidence for the reprotonation of the Schiff base in M_1 from EC, probably followed by a thermal reisomerization to bR_{trans}. In an earlier paper (Butt et al., 1989), it was shown by photoelectrical experiments that in mutant D85E the deprotonation rate is increased by a factor of 5, which could be explained by the increased pK of the carboxylic group of the glutamate. This is consistent with our interpretation and with data from Heberle et al. (1993), who showed a slower proton ejection to the extracellular medium in the mutant D85E, although an additional feedback mechanism between Asp^{85} and the proton uptake pathway was also postulated.

The interpretation of the voltage dependence and the blue light quenching effect results in some interesting conclusions (Fig. 3 *a,b*):

1. A transient current precedes the stationary pump current at negative potentials. This is in agreement with a fast electrogenic proton release via EC preceding the slow reuptake of protons from the same side in the M_1 state, which is accumulated by the negative potential. At positive potentials, no transient currrents can be observed. Under these conditions the branching of the transport cycle becomes negligible, and the M-to-ground state reaction becomes faster than the absorption of photons at nonsaturating light conditions (Fendler et al., 1987).

2. At negative potentials, blue light induces a transient current directed against the normal pump direction. This can be explained by the accumulation of M_1, where the blue light induces the $M_{cis} \rightarrow M_{trans}$ isomerization with proton uptake from EC. The larger the inhibiting potential, the larger the amount of M_1, so that the transient current can cross the zero line. As can be seen in Fig. 3 *a*, at -160 mV, the stationary pump current becomes virtually zero under simultaneous application of red and blue light, but it does not invert, as was shown recently for the bR mutant D85T (Tittor et al., 1994). Transport models with a molecular switch of accessibility (Oesterhelt et al., 1992; Lanyi, 1995; Haupts et al., 1997) predict this behavior, because the Schiff base can only interact with the extracellular half-channel, so that net transport of protons in either direction becomes impossible, because the potential blocks the switch of accessibility.

3. Although the main electrogenic event in the transport cycle was attributed to the M decay, the photocurrent is mainly influenced by the ratio of M_1/M_2, allowing at negative potentials the parallel nontransporting cycle. The underlying process of this voltage dependence is unknown. However, our finding that negative potentials arrest the protein in M_1 suggests that the M_1-M_2 transition (the switch) is a part of the electrogenic event during the M-decay. A similar conclusion was recently obtained in a structural study on bR, postulating that tertiary structural changes between M_1 and M_2 are responsible for the switch and are triggered by a charge redistribution (Sass et al., 1997). Positive potentials would diminish the M_1 concentration, thereby reducing the branching into the nontransporting cycle. It is noteworthy to say that the accumulation of M_1 by the electric field opens the possibility of studying the structure of the protein in this conformation by the appropriate methods. This would give valuable information about the switch, the crucial step in the pumping cycle. The demonstration of the activation of a parallel nontransporting cycle is an interesting alternative to the current models for the regulation of an ion pump by the electric field.

The authors thank A. Becker and D. Stiegert for excellent technical assistance; W. Stoeckenius and K. Fendler for valuable discussions; R. Clarke for critical reading of the manuscript; and D. Oesterhelt and J.

Tittor, Max Planck Institute for Biochemistry, Martinsried, for providing us with purple membranes containing wt-bR or the mutant D85E.

This work was supported by the Deutsche Forschungsgemeinschaft (SFB 169).

REFERENCES

Bamberg, E., H. J. Apell, N. A. Dencher, W. Sperling, H. Stieve, and P. Läuger. 1979. Photocurrents generated by bacteriorhodopsin on planar bilayer membranes. *Biophys. Struct. Mech.* 5:277–292.

Bamberg, E., N. A. Dencher, A. Fahr, and M. P. Heyn. 1980. Transmembraneous incorporation of photoelectrically active bacteriorhodopsin in planar lipid bilayers. *Proc. Natl. Acad. Sci. USA.* 78:7502–7506.

Bamberg, E., J. Tittor, and D. Oesterhelt. 1993. Light-driven proton or chloride pumping by halorhodopsin. *Proc. Natl. Acad. Sci. USA.* 90: 639–643.

Birnboim, H. C., and J. Doly. 1979. A rapid alkaline extraction procedure for screening recombinant plasmid DANN. *Nucleic Acids Res.* 7:1513–1523.

Braun, D., N. A. Dencher, A. Fahr, M. Lindau, and M. P. Heyn. 1988. Nonlinear voltage dependence of the light-driven proton pump current of bacteriorhodopsin. *Biophys. J.* 53:617–621.

Butt, H. J., K. Fendler, E. Bamberg, J. Tittor, and D. Oesterhelt. 1989. Aspartic acids 96 and 85 play a central role in the function of bacteriorhodopsin as a proton pump. *EMBO J.* 8:1657–1663.

Dancsházy, Z., and B. Karvalyi. 1976. Incorporation of bacteriorhodopsin into a bilayer lipid membrane: a photoelectric-spectroscopic study. *FEBS Lett.* 72:136–138.

Drachev, D. A., A. D. Kaulen, L. V. Khitrina, and V. P. Skulachev. 1981. Fast stages of photoelectric processes in biological membranes. I. Bacteriorhodopsin. *Eur. J. Biochem.* 117:461–470.

Druckmann, S., M. Ottolenghi, A. Pande, J. Pande, and R. H. Callunder. 1982. Acid-base equilibrium of the Schiff base in bacteriorhodopsin. *Biochemistry.* 21:4953–4959.

Dubrovskii, F. T., S. P. Balashov, O. A. Sineshchekov, L. N. Chekulaeva, and F. F. Litvin. 1982. Photoinduced changes in the quantum yields of the photochemical cycle of conversions of bacteriorhodopsin and transmembrane transport of protons in *Halobacterium halobium* cells. *Biokhimiya.* 47:1230–1240.

Fahr, A., P. Läuger, and E. Bamberg. 1981. Photocurrent kinetics of purple-membrane sheets bound to planar bilayer membranes. *J. Membr. Biol.* 60:51–62.

Fendler, K., W. Gärtner, D. Oesterhelt, and E. Bamberg. 1987. Electrogenic transport properties of bacteriorhodopsin containing chemically modified retinal analogues. *Biochim. Biophys. Acta.* 893:60–68.

Gerwert, K., G. Souvignier, and B. Hess. 1990. Simultaneous monitoring of light-induced changes in protein side-group protonation chromophore isomerization and backbone motion of bacteriorhodopsin by time-resolved Fourier-transform IR spectroscopy. *Proc. Natl. Acad. Sci USA.* 87:9774–9778.

Grigorieff, N., T. A. Ceska, K. H. Downing, J. M. Baldwin, and R. Henderson. 1996. Electron-crystallographic refinement of the structure of bacteriorhodopsin. *J. Mol. Biol.* 259:393–421.

Groma, G. I., S. L. Helgerson, P. K. Wolber, D. Beece, Zs. Dancshazy, L. Keszthelyi, and W. Stoeckenius. 1984. Coupling between the bacteriorhodopsin photocycle and the protonmotive force in *Halobacterium halobium* cell envelope vesicles. II. Quantitation and preliminary modeling of the M → bR reactions. *Biophys. J.* 45:985–992.

Grygorczyk, R., P. Hanke-Baier, W. Schwarz, and H. Passow. 1989. Measurement of erythroid band 3 protein-mediated anion transport in mRNA injected oocytes of *Xenopus laevis*. *Methods Enzymol.* 173: 453–466.

Haupts, U., E. Bamberg, and D. Oesterhelt. 1996. Different modes of proton translocation by sensory rhodopsin I. *EMBO J.* 15:1834–1841.

Haupts, U., J. Tittor, E. Bamberg, and D. Oesterhelt. 1997. General concept for ion translocation by halobacterial retinal proteins: the isomerisation/switch/transfer (IST) model. *Biochemistry.* 36:2–7.

Heberle, J., D. Oesterhelt, and N. A. Dencher. 1993. Decoupling of photo- and proton cycle in the Asp^{85}→Glu mutant of bacteriorhodopsin. *EMBO J.* 12:3721–3727.

Hellingwerf, K. J., J. J. Schuurmans, and H. V. Westerhoff. 1978. Demonstration of coupling between the protonmotive force across bacteriorhodopsin and the flow through its photochemical cycle. *FEBS Lett.* 92:181–186.

Henderson, R., J. M. Baldwin, T. A. Ceska, F. Zemlin, E. Beckmann, and K. H. Downing. 1990. Model for the structure of bacteriorhodopsin based on high-resolution electron cryo-microscopy. *J. Mol. Biol.* 213: 899–929.

Hildebrandt, V., K. Fendler, J. Heberle, A. Hoffmann, E. Bamberg, and G. Büldt. 1993. Bacteriorhodopsin expressed in *Schizosaccharomyces pombe* pumps protons through the plasma membrane. *Proc. Natl. Acad. Sci. USA.* 90:3578–3582.

Keszthelyi, L., and P. Ormos. 1980. Electric signals associated with the photocycle of bacteriorhodopsin. *FEBS Lett.* 109:189–193.

Koch, M. H., N. A. Dencher, D. Oesterhelt, H. J. Plohn, G. Rapp, and G. Buldt. 1991. Time-resolved x-ray diffraction study of structural changes associated with the photocycle of bacteriorhodopsin. *EMBO J.* 10: 521–526.

Korenstein, R., B. Hess, and D. Kuschmitz. 1978. Branching reactions in the photocycle of bacteriorhodopsin. *FEBS Lett.* 93:266–270.

Lanyi, J. K. 1995. Bacteriorhodopsin as a model for proton pumps. *Nature.* 375:461–463.

Lanyi, J. K., and G. Váró. 1995. The photocycles of bacteriorhodopsin. *Isr. J. Chem.* 35:365–385.

Lukashev, E. P., E. Vozary, A. A. Kononenko, and A. B. Rubin. 1980. Electric field promotion of the bacteriorhodopsin BR_{570} to BR_{412} photoconversion in films of *Halobacterium halobium* purple membranes. *Biochim. Biophys. Acta.* 592:258–266.

Mathies, R. A., S. W. Lin, J. B. Ames, and W. T. Pollard. 1991. From femtoseconds to biology: mechanisms of bacteriorhodopsin's light-driven proton pump. *Annu. Rev. Biophys. Chem.* 20:491–518.

Michel, H., and D. Oesterhelt. 1976. Light-induced changes of the pH gradient and the membrane potential in *Halobacterium halobium. FEBS Lett.* 65:175–178.

Nagel, G., B. Möckel, G. Büldt, and E. Bamberg. 1995. Functional expression of bacteriorhodopsin in oocytes allows direct measurement of voltage dependence of light induced H^+ pumping. *FEBS Lett.* 377: 263–266.

Oesterhelt, D., and B. Hess. 1973. Reversible photolysis of the purple complex in the purple membrane of *Halobacterium halobium*. *Eur. J. Biochem.* 37:316–326.

Oesterhelt, D., J. Tittor, and E. Bamberg. 1992. A unifying concept for ion translocation by retinal proteins. *J. Bioenerg. Biomembr.* 24:181–191.

Ormos, P., Z. Dancshazy, and B. Karvaly. 1978. Mechanism of generation and regulation of photopotential by bacteriorhodopsin in bimolecular lipid membrane: the quenching effect of blue light. *Biochim. Biophys. Acta.* 503:304–315.

Ormos, P., Z. Dancshazy, and L. Keszthelyi. 1980. Electric response of a back photoreaction in the bacteriorhodopsin photocycle. *Biophys. J.* 31:207–213.

Quintanilha, A. T. 1980. Control of the photocycle in bacteriorhodopsin by electrochemical gradients. *FEBS Lett.* 117:8–12.

Richter, H-T., L. S. Brown, R. Needleman, and J. K. Lanyi. 1996a. A linkage of the pK_a's of asp-85 and glu-204 forms part of the reprotonation switch of bacteriorhodopsin. *Biochemistry.* 35:4054–4062.

Richter, H-T., R. Needleman, and J. K. Lanyi. 1996b. Perturbed interaction between residues 85 and 204 in tyr-185→phe and asp-85→glu bacteriorhodopsins. *Biophys. J.* 71:3392–3398.

Sass, H. J., I. W. Schachowa, G. Rapp, M. H. Koch, D. Oesterhelt, N. A. Dencher, and G. Büldt. 1997. The tertiary structural changes in bacteriorhodopsin occur between M states: x-ray diffraction and Fourier transform infrared spectroscopy. *EMBO J.* 16:1484–1491.

Schulten, K., and P. Tavan. 1978. A mechanism for the light-driven proton pump of *Halobacterium halobium*. *Nature.* 272:85–86.

Sheves, M., A. Albeck, N. Friedman, and M. Ottolenghi. 1986. Controlling the pK_a of the bacteriorhodopsin Schiff base by use of artificial retinal analogues. *Proc. Natl. Acad. Sci. USA.* 83:3262–3266.

Tittor, J., U. Schweiger, D. Oesterhelt, and E. Bamberg. 1994. Inversion of proton translocation in bacteriorhodopsin mutants D85N, D85T, and D85,96N. *Biophys. J.* 67:1682–1690.

Váró, G., and L. Keszthelyi. 1983. Photoelectric signals from dried oriented purple membranes of *Halobacterium halobium*. *Biophys. J.* 43:47–51.

Váró, G., and K. J. Lanyi. 1991a. Kinetic and spectroscopic evidence for an irreversible step between deprotonation and reprotonation of the Schiff base in the bacteriorhodopsin photocycle. *Biochemistry.* 30: 5008–5015.

Váró, G., and K. J. Lanyi. 1991b. Thermodynamics and energy coupling in the bacteriorhodopsin photocycle. *Biochemistry.* 30:5016–5022.

Westerhoff, H. V., and Zs. Dancsházy. 1984. Keeping a light-driven proton pump under control. *Trends Biochem. Sci.* 9:112–116.